

## Dynamics of nitrate production and removal as a function of residence time in the hyporheic zone

Jay P. Zarnetske,<sup>1</sup> Roy Haggerty,<sup>1</sup> Steven M. Wondzell,<sup>2</sup> and Michelle A. Baker<sup>3</sup>

Received 18 March 2010; revised 7 December 2010; accepted 21 December 2010; published 10 March 2011.

[1] Biogeochemical reactions associated with stream nitrogen cycling, such as nitrification and denitrification, can be strongly controlled by water and solute residence times in the hyporheic zone (HZ). We used a whole-stream steady state <sup>15</sup>N-labeled nitrate (<sup>15</sup>NO<sub>3</sub><sup>-</sup>) and conservative tracer (Cl<sup>-</sup>) addition to investigate the spatial and temporal physiochemical conditions controlling the denitrification dynamics in the HZ of an upland agricultural stream. We measured solute concentrations (<sup>15</sup>NO<sub>3</sub><sup>-</sup>, <sup>15</sup>N<sub>2</sub> (g), as well as NO<sub>3</sub><sup>-</sup>, NH<sub>3</sub>, DOC, DO, Cl<sup>-</sup>), and hydraulic transport parameters (head, flow rates, flow paths, and residence time distributions) of the reach and along HZ flow paths of an instrumented gravel bar. HZ exchange was observed across the entire gravel bar (i.e., in all wells) with flow path lengths up to 4.2 m and corresponding median residence times greater than 28.5 h. The HZ transitioned from a net nitrification environment at its head (short residence times) to a net denitrification environment at its tail (long residence times). NO<sub>3</sub><sup>-</sup> increased at short residence times from 0.32 to 0.54 mg-N L<sup>-1</sup> until a threshold of 6.9 h and then consistently decreased from 0.54 to 0.03 mg-N L<sup>-1</sup>. Along these same flow paths, declines were seen in DO (from 8.31 to 0.59 mg-O<sub>2</sub> L<sup>-1</sup>) and DOC (from 3.0 to 1.7 mg-C L<sup>-1</sup>). The rates of the DO and DOC removal and net nitrification were greatest during short residence times, while the rate of denitrification was greatest at long residence times. <sup>15</sup>NO<sub>3</sub><sup>-</sup> tracing confirmed that a fraction of the NO<sub>3</sub><sup>-</sup> removal was via denitrification as <sup>15</sup>N<sub>2</sub> was produced across the entire gravel bar HZ. Production of <sup>15</sup>N<sub>2</sub> across all observed flow paths and residence times indicated that denitrification microsites are present even where nitrification was the net outcome. These findings demonstrate that the HZ is an active nitrogen sink in this system and that the distinction between net nitrification and denitrification in the HZ is a function of residence time and exhibits threshold behavior. Consequently, incorporation of HZ exchange and water residence time characterizations will improve mechanistic predictions of nitrogen cycling in streams.

**Citation:** Zarnetske, J. P., R. Haggerty, S. M. Wondzell, and M. A. Baker (2011), Dynamics of nitrate production and removal as a function of residence time in the hyporheic zone, *J. Geophys. Res.*, 116, G01025, doi:10.1029/2010JG001356.

### 1. Introduction

[2] Surplus nitrogen adversely affects aquatic systems, contributing to extensive surface and groundwater degradation, which is a persistent and growing global problem [Schlesinger *et al.*, 2006; Diaz and Rosenberg, 2008]. Stream ecosystems can be important locations of N retention along the continuum between terrestrial and ocean environments. Research has established that headwater and mid-network streams are most effective at regulating downstream

nitrogen exports [Peterson *et al.*, 2001; Alexander *et al.*, 2000; Mulholland *et al.*, 2008]. These same small streams are also where stream-groundwater (hyporheic, HZ) flux is greatest relative to surface flux [Anderson *et al.*, 2005]. Previous work clearly shows that HZ exchange can regulate nitrogen [Holmes *et al.*, 1996; Wondzell and Swanson, 1996; Hill and Lyburner, 1998]. However, the linkages between HZ hydrology and stream nitrogen export are poorly understood and there is no clear mechanistic representation of HZ controls on nitrogen flux through streams [Duff and Triska, 2000; Böhlke *et al.*, 2009]. Hence, there is a need to quantify the coupling of HZ hydrology and biogeochemical conditions and their role in creating stream nitrogen sources and sinks. Until the linkages between HZ hydrology and nitrogen biogeochemistry are established, it will be unclear how the HZ influences nitrogen dynamics at reach and catchment scales. In this study we move toward this mechanistic understanding of nitrogen fate and transport by

<sup>1</sup>Department of Geosciences and Water Resources Graduate Program, Oregon State University, Corvallis, Oregon, USA.

<sup>2</sup>Olympia Forestry Sciences Laboratory, Pacific Northwest Research Station, Olympia, Washington, USA.

<sup>3</sup>Department of Biology and the Ecology Center, Utah State University, Logan, Utah, USA.

observing and relating the HZ residence timescales to N transformations.

[3] There are many processes that temporarily remove or relocate inorganic N from stream water (e.g., sorption onto substrate, assimilation into plants or microbes), but denitrification is the primary mechanism by which inorganic N is permanently removed from the stream system. Consequently, denitrification has been the source of significant research because of its potential role in regulating the downstream transport of inorganic N. Denitrification in streams is primarily regulated by redox conditions,  $\text{NO}_3^-$  concentrations, and labile dissolved organic carbon (DOC) availability [Holmes *et al.*, 1996; Duff *et al.*, 1996; Baker *et al.*, 1999]. The HZ is known to create strong gradients in each of these conditions regulating nitrogen cycling [Triska *et al.*, 1993; Jones and Holmes, 1996; Hill and Lymburner, 1998; Hedin *et al.*, 1998]. Consequently, the HZ has been identified as a potential hot spot for denitrification in aquatic systems [McClain *et al.*, 2003]. However, the HZ is not simply a net sink (via denitrification), it can also be a source (via nitrification) of nitrate where ever nitrification exceeds denitrification [Jones *et al.*, 1995]. The nitrate produced in the HZ can fuel primary production in surface waters [Valett *et al.*, 1994; Henry and Fisher, 2003].

[4] The role each HZ plays in regulating downstream nitrogen export is variable in space and time [e.g., Wondzell and Swanson, 1996]. This is due to the temporal and spatial variation in substrate and transport limitations on nitrogen transformations. For example substrate limitations acting on denitrification, such as the type and quantity of nitrogen and DOC entering the HZ, can vary significantly in time (e.g., seasonally [Kaplan and Newbold, 2000]). On the other hand, physical transport conditions of the HZ, which are a function of energy gradients and hydraulic conductivity, will regulate the rate at which nitrogen, dissolved oxygen (DO), and DOC are supplied to the sediment [Baker *et al.*, 2000]. For example, DO exerts a strong control on nitrogen dynamics in the HZ, and research has shown that DO dynamics are related to water residence time in the HZ [Triska *et al.*, 1993; Findlay, 1995; Valett *et al.*, 1996; Morrice *et al.*, 2000]. Recently, research has started to integrate physical transport and biogeochemical approaches to assess HZ denitrification as a function of HZ residence time [e.g., Gu *et al.*, 2007; Clilverd *et al.*, 2008; Pinay *et al.*, 2009]. The use of  $^{15}\text{N}$  tracers has also advanced our understanding of aquatic N cycling. Böhlke *et al.* [2004, 2009] and Mulholland *et al.* [2004, 2008] demonstrated the usefulness of the field  $^{15}\text{N}$  tracer approach for determining denitrification rates of streams at the reach scale. Böhlke *et al.* [2004, 2009], in particular, showed that the key sources of uncertainty in measuring reach denitrification with traditional mass balance approaches, nitrification and nitrate uptake, can be accounted for with the use of  $^{15}\text{N}$  tracer approach. Although many advances about nitrogen cycling in streams have resulted from this  $^{15}\text{N}$  tracer work, these studies were unable to account for the entire nitrogen budget in streams. Böhlke *et al.* [2004] and Mulholland *et al.* [2004, 2008] suggest that a portion of the unaccounted for nitrogen may be due to benthic and hyporheic nitrogen retention and removal processes. Recently, Böhlke *et al.* [2009] demonstrated with whole stream  $^{15}\text{NO}_3^-$  addition experiments that between 14 and

97% of whole stream denitrification was attributed to HZ denitrification.

[5] The objective of this study was to assess the substrate and transport conditions controlling net HZ denitrification. We hypothesize that biogeochemical reactions associated with stream nitrogen cycling, such as nitrification and denitrification are strongly controlled by water residence times in the HZ. To test the hypothesis, we conducted a whole-stream steady state  $^{15}\text{NO}_3^-$  and a conservative tracer experiment in an upland agricultural stream to measure the in situ spatial and temporal hydraulic and biogeochemical conditions controlling HZ nitrification and denitrification. We show here that  $^{15}\text{NO}_3^-$  tracing techniques characterize HZ denitrification and that the conditions conducive to net denitrification vary with subsurface residence times. Ultimately, relating HZ denitrification controls to residence times will help to upscale denitrification measurements to reach and network scales in a way that is linked quantitatively to transient storage.

## 2. Methods

### 2.1. Study Site

[6] The study site consists of a 303 m reach containing an instrumented gravel bar hyporheic zone on Drift Creek (Figure 1a), a third-order stream within the Willamette River basin in western Oregon, USA (44.9753°N, 122.8259°W). The drainage area above the study reach is 6517 ha, and has mixed land use dominated by agriculture (lower catchment) and forestry (upper catchment). The catchment population is predominantly rural with septic systems, another potential source of N in the study stream. Annual precipitation is 1190 mm and comes primarily during the winter as rain. Base flow discharge gradually decreases to an annual minimum ( $<50 \text{ L s}^{-1}$ ) in early September. The study reach was modified by channelization in the past, as were many of the streams in this agricultural region. The channelized stream is incised into competent bedrock consisting of andesite flow breccias and is now separated from an active floodplain. The incised active channel is 10–20 m wide and is bounded by steep banks 3–5 m high. The alluvial thickness above bedrock (as depth to refusal) varies from 0 to  $\geq 1.5$  m. Consequently, the reach has a limited and constrained hyporheic zone. The study reach has a slope of  $0.007 \text{ m m}^{-1}$  and the morphology is primarily a planebed channel with occasional pool-riffle sequences (see Montgomery and Buffington [1997] for definitions of channel types). The streambed consists of poorly sorted sand, gravel, cobbles, and boulders.

[7] The hyporheic zone study site is a lateral gravel bar approximately 6.1 m by 4 m (Figure 1b). This gravel bar is adjacent to a riffle on one side and connected to the bedrock channel bank on the other side. The gravel bar separates two pools and spans a head loss across the riffle of 0.13 m. The alluvium comprising this gravel bar was uniformly 1.2 m thick. The observed and modeled subsurface exchange across this gravel bar primarily occurs along lateral flow paths from the head to the tail of the bar (Figure 1b). This gravel bar was instrumented with a well network ( $n = 11$ ) of 3.8 cm I.D. schedule 40 PVC wells screened 0.2–0.4 m below ground surface. Chloride ( $\text{Cl}^-$ ) tracer tests conducted prior to the experiment demonstrated that all wells were

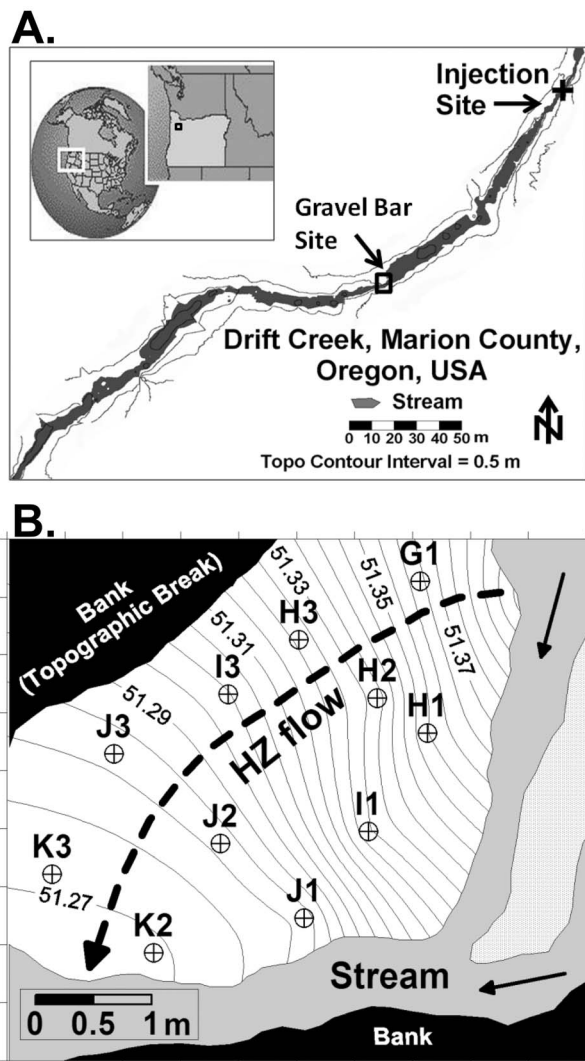


**Figure 1.** (a) Map of the Drift Creek study site showing tracer injection site and the gravel bar hyporheic site. (b) Map of the hyporheic study site showing locations of wells (dots with cross hairs) and water potentiometric surface during the injection experiment. Stream briefly bifurcates near gravel bar (i.e., not a tributary confluence), and water chemistry is the same across channel. Dashed arrow indicates a single representative simulated flow path between the head and tail of the gravel bar.

connected to stream water and that well water originated from the stream and not from the groundwater aquifer. This lack of groundwater inflows reduces the uncertainty of  $^{15}\text{N}$  tracing interpretation in this HZ system; groundwater inflow of nitrogen is a common source of uncertainty seen in other systems [e.g., Böhlke *et al.*, 2004]. Background stream and hyporheic biogeochemistry are presented in Table 1.

## 2.2. Field Procedures

[8] We performed a whole-stream steady state  $\delta^{15}\text{NO}_3^-$  and conservative tracer ( $\text{Cl}^-$ ) injection on 23–24 August 2007 when discharge was relatively stable. Following methods from Mulholland *et al.* [2004], an injection solu-

tion of  $\delta^{15}\text{NO}_3^-$  (as 99% enriched  $\text{K}^{15}\text{NO}_3$ ) and  $\text{Cl}^-$  (as  $\text{NaCl}$ ) was released at a constant rate ( $154 \text{ mL min}^{-1}$ ) using a peristaltic pump at the head of the reach for 27.5 h starting at 1428 h (Geopump Series I, Geotech Environmental Equipment, Denver, Colorado, USA, note that the use of trade names in this publication is for reader information and does not imply endorsement by the U.S. Department of Agriculture of any product or service). The amount of  $\text{K}^{15}\text{NO}_3$  introduced to the reach was calculated to produce a target  $\delta^{15}\text{N}$  enrichment of 10 000‰ in the stream water  $\text{NO}_3^-$ . The  $\text{Cl}^-$  mass addition target was to elevate the background stream  $\text{Cl}^-$  400% and generate an electrical conductivity increase of 50%. The solution was injected into a turbulent riffle sufficiently upstream of the first sampling location to guarantee complete lateral and vertical channel mixing at all downstream sampling locations. The  $\text{K}^{15}\text{NO}_3$  addition produced a 3% increase in ambient stream  $\text{N-NO}_3^-$ .

[9] Electrical conductivity was used to measure the real-time  $\text{Cl}^-$  transport through the stream and hyporheic zone. The electrical conductivity measurements were taken every 60 s in all 11 wells and in the stream water at the head and tail of the gravel bar. These electrical conductivity measurements were made with 13 multiplexed, in situ, CS547A conductivity and temperature probes connected to a CR1000 (Campbell Scientific, Logan, Utah, USA). The  $\text{Cl}^-$  transport at the end of the experimental reach was captured via automated sampling every 10 min until plateau and then every 2 h during plateau (ISCO model 3700, Lincoln, Nebraska, USA) and subsequently field measured with an electrical conductivity meter (YSI model 63, Yellow Springs, Ohio, USA). These electrical conductivity measurements were used to characterize the solute transport dynamics including flow rates, flow paths, and residence times as well as to inform the timing of the sampling regime described below.

[10] The water sampling regime consisted of collecting multiple rounds of stream and hyporheic samples during the two phases of the experiment: preinjection and plateau (steady state). For each location (11 wells plus stream water at the gravel bar head), repeated sampling occurred during the preinjection ( $n = 3$ ) and plateau ( $n = 5$ ) periods (Figure 2). The plateau sampling period was initiated at 22.5 h after injection when all hyporheic wells demonstrated near steady state electrical conductivity. Repeated hyporheic samples were collected approximately every 1 h during the plateau period.

[11] Water samples were collected for key solute concentrations and  $\delta^{15}\text{N}$  enrichments relevant to the respiratory denitrification process ( $\delta^{15}\text{NO}_3^-$ ,  $\delta^{15}\text{N}_2$  (g), as well as  $\text{NO}_3^-$ ,  $\text{NH}_3$ , DOC, DO,  $\text{Cl}^-$ , and specific ultraviolet absorption ( $\text{SUVA}_{254}$ ). Hyporheic well samples were collected with a field peristaltic pump (Masterflex L/S, Vernon Hills, Illinois, USA) [Woessner, 2007]. All water samples were immediately filtered through ashed Whatman GF/F glass fiber filters ( $0.7 \mu\text{m}$  pore size) into acid washed HDPE bottles (60 mL for nutrient chemistry and 1 L for  $^{15}\text{N}$  isotope samples). Following filtering, nutrient chemistry samples and isotope samples were stored on ice in the field and later refrigerated at  $4^\circ\text{C}$  or frozen in the laboratory until processed and analyzed. DO concentrations were measured in situ with a calibrated YSI DO Meter (Model 52) at all locations prior to collecting each round of samples. Samples were also collected for  $\delta^{15}\text{N}_2\text{O}$  (g), but were unable to be

**Table 1.** Background Stream and Hyporheic Biogeochemistry<sup>a</sup>

Site	DO (mg-O <sub>2</sub> L <sup>-1</sup> )	NO <sub>3</sub> <sup>-</sup> (mg-N L <sup>-1</sup> )	NH <sub>3</sub> (mg-N L <sup>-1</sup> )	DOC (mg-C L <sup>-1</sup> )	$\delta^{15}\text{N-NO}_3^-$ (‰ Versus AIR)	$\delta^{15}\text{N-N}_2$ (‰ Versus AIR)
Stream	8.31 ± 0.43	0.32 ± 0.01	0.02 ± 0.02	3.01 ± 0.15	2.19 ± 0.61	3.00 ± 0.37
G1	2.07 ± 0.05	0.54 ± 0.06	0.11 ± 0.02	2.07 ± 0.15	5.48 ± 3.33	1.20 ± 0.61
H1	3.27 ± 0.09	0.43 ± 0.05	0.05 ± 0.01	2.18 ± 0.14	5.35 ± 2.27	0.80 ± 0.61
H2	1.30 ± 0.03	0.27 ± 0.03	0.06 ± 0.01	2.01 ± 0.17	5.00 ± 3.26	0.50 ± 1.01
H3	0.72 ± 0.06	0.33 ± 0.03	0.05 ± 0.01	2.01 ± 0.20	14.92 ± 2.25	0.60 ± 1.10
I1	1.09 ± 0.05	0.25 ± 0.04	0.08 ± 0.01	1.94 ± 0.15	18.10 ± 2.88	1.50 ± 0.79
I3	0.93 ± 0.09	0.13 ± 0.00	0.07 ± 0.01	1.98 ± 0.10	14.18 ± 1.99	2.80 ± 0.61
J1	0.70 ± 0.06	0.07 ± 0.02	0.01 ± 0.01	1.66 ± 0.12	4.03 ± 2.18	0.30 ± 3.18
J2	0.61 ± 0.09	0.13 ± 0.01	0.02 ± 0.01	1.79 ± 0.10	8.85 ± 2.30	2.30 ± 0.87
J3	0.51 ± 0.05	0.11 ± 0.01	0.04 ± 0.01	1.76 ± 0.08	11.35 ± 2.13	3.30 ± 3.46
K2	0.65 ± 0.05	0.08 ± 0.01	0.04 ± 0.01	1.71 ± 0.06	8.13 ± 2.25	0.00 ± 2.82
K3	0.59 ± 0.10	0.09 ± 0.01	0.02 ± 0.01	1.70 ± 0.11	10.25 ± 2.96	0.00 ± 0.37

<sup>a</sup>Mean of three observations before injection ± 1 standard error.

analyzed due to technical problems at the stable isotope laboratory. However, denitrification in freshwater and nearshore marine system sediments consists almost entirely of N<sub>2</sub> production with N<sub>2</sub>O/N<sub>2</sub> production ratios generally between < 0.001 and < 0.05 [Seitzinger, 1988; Mulholland et al., 2004], so <sup>15</sup>N<sub>2</sub> by itself is capable of characterizing the majority of the denitrification dynamics.

[12] The <sup>15</sup>N gas collection for each sample occurred in the field and followed procedures adapted from Hamilton and Ostrom [2007]. A peristaltic pump was used to collect 80 mL water samples into a 140 mL plastic syringe (Becton-Dickinson, Franklin Lakes, NJ, USA) fitted with stopcocks. All visible bubbles were expelled so that there was no headspace. To avoid any atmospheric N contamination, sample syringes were submerged under water in a processing tub kept at stream temperature. An underwater transfer of 40 mL high purity He was added to each sample syringe. Sample syringes were then gently shaken for 10 min to permit equilibration of the N<sub>2</sub> (g) into the He headspace. Following equilibration, approximately 14 mL of headspace gas was then injected into preevacuated 12 mL exetainers (Labco Limited, Wycombe, UK). Exetainers were preevacuated by pumping them down to a pressure of <50 mTorr using a Welch vacuum pump (Model DirectTorr 8905, Skokie, Illinois, USA) and then stored underwater in He purged DI water-filled centrifuge tubes until sample collection. Sample-filled exetainers were then returned to their zero headspace He purged DI water-filled centrifuge tubes for storage until analysis.

[13] Following the experiment (5–6 Sept. 2007) and during similar stable low flow conditions, we collected detailed thalweg surface water and channel surface topography data for the reach using a Topcon total station (Model GTS-226, Livermore, California, USA) and standard surveying methods with spatial resolution of  $x \leq 1$  m,  $y \leq 1$  m,  $z \leq 0.01$  m for the greater reach and  $x \leq 0.1$  m,  $y \leq 0.1$  m,  $z \leq 0.005$  m for the instrumented gravel bar site.

### 2.3. Laboratory Procedures

[14] Stream and hyporheic samples were analyzed for NO<sub>3</sub><sup>-</sup>, NH<sub>3</sub>, DOC, and Cl<sup>-</sup> at the Cooperative Chemical Analytical Laboratory (Corvallis, Oregon, USA). The NO<sub>3</sub><sup>-</sup> and NH<sub>3</sub> measurements were made by a Technicon Auto-Analyzer II. The NO<sub>3</sub><sup>-</sup> and NH<sub>3</sub> nutrient analyses were performed following standard colorimetric methodology and

had detection limits of 0.001 mg L<sup>-1</sup> and 0.01 mg L<sup>-1</sup>, respectively. The concentration of total DOC was determined with a Shimadzu TOC-VCSH Combustion Analyzer (Tokyo, Japan; detection limit = 0.05 mg L<sup>-1</sup>). The Cl<sup>-</sup> was determined by ion chromatography (Dionex 1500, Sunnyvale, California, USA; detection limit = 0.01 mg L<sup>-1</sup>). SUVA values were determined by dividing the UV absorbance measured at  $\lambda = 254$  nm by the DOC concentration and are reported in the units of liter per milligram carbon per meter [Weishaar et al., 2003].

[15] The  $\delta^{15}\text{N}$  content of the stream and hyporheic water NO<sub>3</sub><sup>-</sup> was determined by methods adapted from Sigman et al. [1997] and Mulholland et al. [2004], which are briefly summarized below. Prior to  $\delta^{15}\text{N}$  analysis, <sup>15</sup>NO<sub>3</sub><sup>-</sup> samples with blanks and standards were processed in the following manner. First, a volume of each sample (0.25–1 L; processing volume is dependent on N content of each sample) was stripped of its dissolved NH<sub>4</sub><sup>+</sup> and had its NO<sub>3</sub><sup>-</sup> concentrated. Second, the concentrated sample NO<sub>3</sub><sup>-</sup> was captured on a prepared filter via a reduction/diffusion/sorption

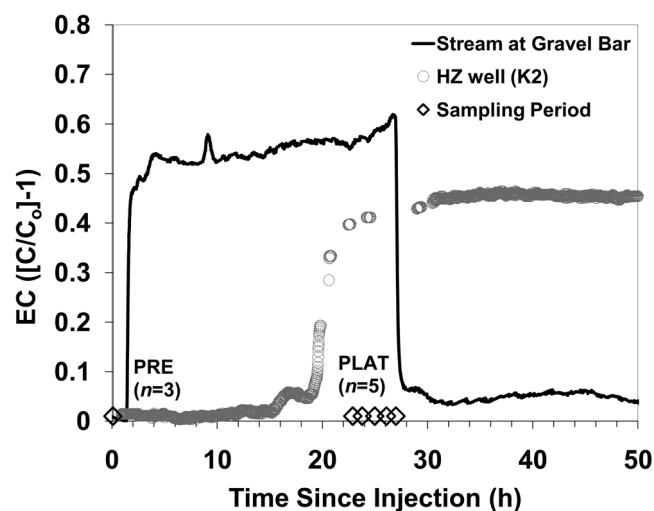


**Figure 2.** The stream at gravel bar and representative distal HZ well (K2) electrical conductivity (EC) breakthrough curves showing the timing of the repeated preinjection and plateau sampling events. Gaps in well EC data represent times when EC probes were disturbed via sampling.

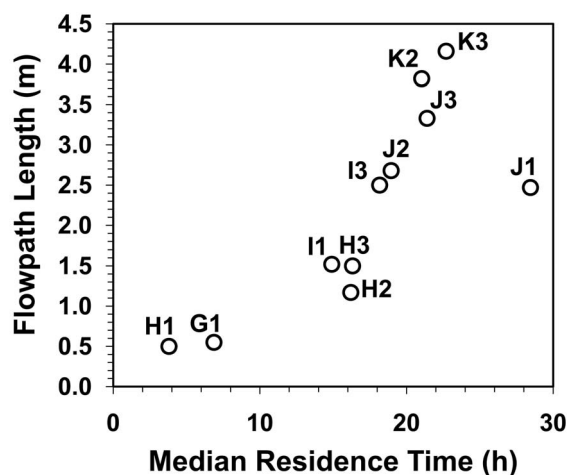


**Figure 3.** Nominal flow path length and median residence time for each hyporheic zone well.

procedure (full reduction of  $\text{NO}_3^-$  to  $\text{NH}_4^+$ , which is then converted to  $\text{NH}_3$  that diffuses into the headspace and ultimately gets captured on the acidified sorption filter). After complete transfer of  $\text{NO}_3^-$  to the sample filter, the samples were sealed and sent for  $^{15}\text{NO}_3^-$  analysis. All  $\delta^{15}\text{NO}_3^-$  and  $\delta^{15}\text{N}$ -gas samples were analyzed by the Marine Biological Laboratory Stable Isotope Facility (MBL, Woods Hole, Massachusetts, USA). Replicate analyses of the water and gas samples show the precision of  $\delta^{15}\text{NO}_3^-$  and  $\delta^{15}\text{N}_2$  isotope measurements is  $\pm 80.0\%$  and  $\pm 0.2\%$ , respectively.

#### 2.4. Parameter Calculations

[16] Electrical conductivity breakthrough curves (as a measure of  $\text{Cl}^-$  transport) at the head of the gravel bar and in each well were used to measure the median residence time of the study reach and the HZ water in each well. The median residence time was calculated as the time required to raise the EC in the well to one half the plateau concentration. In the case of the wells, median residence times were calculated based on the observed  $\text{Cl}^-$  arrival at the gravel bar, not the start of the injection.

[17] To estimate reactive solute transport through and removal by the HZ, we compared the observed  $\text{NO}_3^-$ ,  $\text{NH}_3$ , DO, and DOC concentrations to the conservative tracer concentrations at steady state conditions [after *Morrice et al.*, 2000]. In the absence of biological or chemical removal, the reactive compounds and  $\text{Cl}^-$  transport should be identical. Based upon this assumption, we calculated the  $\text{NO}_3^-$ ,  $\text{NH}_3$ , DO, and DOC concentrations according to the measured  $\text{Cl}^-$  concentrations observed at each well:

$$R_{pred,x,t} = R_{inj,x} \left[ \frac{C_{x,t} - C_{x,t=0}}{C_{inj} - C_{x,t=0}} \right] + R_{x,t=0} \left[ 1 - \frac{C_{x,t} - C_{x,t=0}}{C_{inj} - C_{x,t=0}} \right] \quad (1)$$

where,  $R$  is the solute concentration of interest ( $\text{NO}_3^-$ ,  $\text{NH}_3$ , DO, or DOC),  $C$  is the conservative tracer concentration ( $\text{Cl}^-$ ), and subscripts *pred*, *inj*, *x*, *t* represent predicted well concentration at plateau, injection concentration in the stream, well location, and sample time period, respectively. We then calculated the difference between the measured and

predicted reactive solute concentrations for each well during the plateau conditions. Reactive solute removal occurs when the observed concentration is less than the predicted concentration and production occurs when the observed concentration is greater than the predicted concentration.

### 3. Results

#### 3.1. Stream Hydrology and Chemical Conditions During Experiment

[18] Streamflow conditions were relatively stable over the experiment with a mean flow of  $22 \text{ L s}^{-1}$  and a variance of  $\pm 2.2 \text{ L s}^{-1}$ . This variance in flow did not create any measurable change in the stage of the stream along the reach, near the gravel bar, or in the heads of the gravel bar wells. Surveying of channel topography and geometry yielded a reach mean depth,  $d$ , of 0.23 m and a mean wetted width,  $w$ , of 5.21 m. Repeated measurements of the head at wells (before plateau sampling disturbances) reflected stable surface water elevations as there was no detectable variation during the experiment. Stream and HZ water temperature ranged between 14.1 and 16.5°C during the injection period. Measured surface water nutrient and chemistry conditions were stable across the experiment and did not show diel patterns with  $\text{NO}_3^-$  ( $0.318\text{--}0.325 \text{ mg-N L}^{-1}$ ),  $\text{NH}_3$  ( $0.021\text{--}0.024 \text{ mg-N L}^{-1}$ ), DOC ( $2.95\text{--}3.45 \text{ mg-C L}^{-1}$ ), DO ( $8.10\text{--}8.51 \text{ mg-O}_2 \text{ L}^{-1}$ ), and pH ( $6.65\text{--}6.85$ ).

#### 3.2. Spatial Dynamics of Hyporheic Transport and N Transformation Conditions

[19] Chloride plateau concentration conditions were achieved in all 11 hyporheic wells, demonstrating good connectivity with surface water. Nominal flow path lengths (Figure 3) ranged from 0.5 m (H1) to 4.2 m (K3). The mean DO decreased from  $8.31$  to  $0.59 \text{ mg-O}_2 \text{ L}^{-1}$  along HZ flow paths (Figure 4a) and the mean DOC decreased from  $3.01$  to  $1.7 \text{ mg-C L}^{-1}$  (Figure 4d). The DOC  $\text{SUVA}_{254}$  concentrations were more spatially variable than DOC, indicating that different locations within the HZ had different quantities of aromatic DOC (Figure 4d, contour map), but did generally decrease along flow paths ( $3.22$  to  $0.94 \text{ L mg-C}^{-1} \text{ m}^{-1}$ ). Along flow paths, DO and DOC removal rates were largest in the first 2 m of the flow paths but continued across the entire gravel bar. In contrast, the N species did not consistently decrease along flow paths. Nitrate increased at the proximal end of the flow paths ( $<0.55 \text{ m}$ ) from  $0.34$  to  $0.54 \text{ mg-N L}^{-1}$  and then decreased along the remainder of the flow paths from  $0.54$  to  $0.02 \text{ mg-N L}^{-1}$  (Figure 4b). Similarly,  $\text{NH}_3$  increased from  $0.02$  to  $0.11 \text{ mg-N L}^{-1}$  at the proximal end of the flow paths and then decreased from  $0.11$  to  $0.01 \text{ mg-N L}^{-1}$  along the remainder of the flow paths (Figure 4c).

[20] Tracing of  $^{15}\text{NO}_3^-$  confirmed that a fraction of the  $\text{NO}_3^-$  removal was via denitrification as  $^{15}\text{N}_2$  was produced across the entire gravel bar HZ (Figure 4f). Production of  $^{15}\text{N}_2$  occurred along all portions of the flow paths, even portions characterized by net nitrification (elevated  $\text{NO}_3^-$  and  $\text{NH}_3$ ). Importantly, there was no consistent spatial gradient in the  $^{15}\text{NO}_3^-$  enrichment from proximal to distal ends of the HZ flow paths (Figure 4e) which, if present, would indicate nonsteady state dynamics. Therefore the range of  $^{15}\text{NO}_3^-$

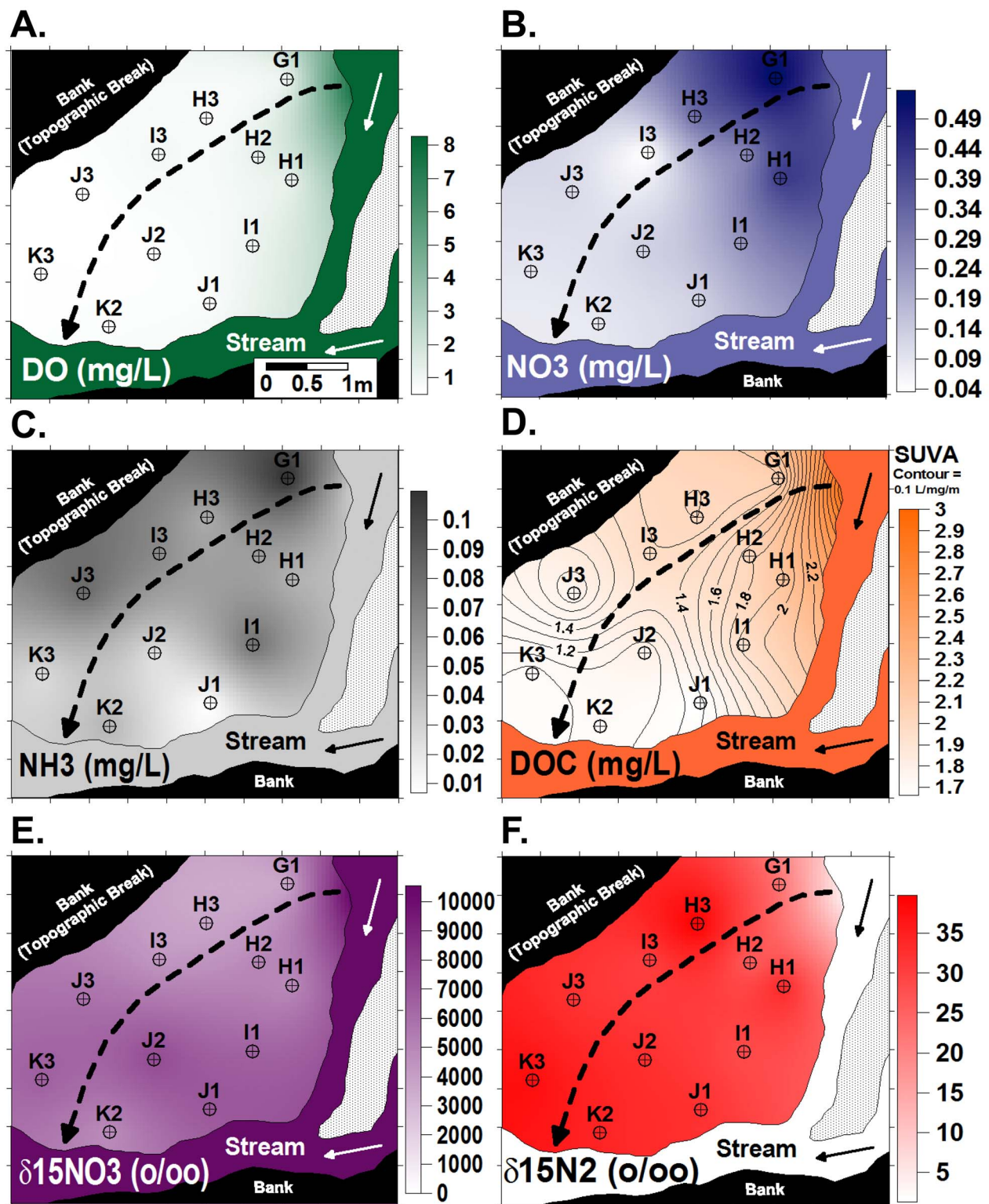


**Figure 4.** Spatial steady state hyporheic zone biogeochemical and  $^{15}\text{N}$  conditions: (a) dissolved oxygen (DO,  $\text{mg-O}_2 \text{ L}^{-1}$ ), (b) nitrate ( $\text{NO}_3^-$ ,  $\text{mg-N L}^{-1}$ ), (c) ammonia ( $\text{NH}_3$ ,  $\text{mg-N L}^{-1}$ ), (d) total dissolved organic carbon (DOC,  $\text{mg-C L}^{-1}$ ) with  $\text{SUVA}_{254}$  contours (interval equals  $0.1 \text{ L mg}^{-1} \text{m}^{-1}$ ), (e)  $\delta^{15}\text{N}$ -nitrate ( $\delta^{15}\text{NO}_3^-$ , ‰ versus AIR), and (f)  $\delta^{15}\text{N}$ -dinitrogen ( $\delta^{15}\text{N}_2$ , ‰ versus AIR). Maps present spatially interpolated mean values generated from repeated samples ( $n = 5$ ) collected during tracer plateau conditions. Stream water values did not vary between the head and tail of the gravel bar.

enrichment is a function of steady state hydrologic and biological conditions. The gravel bar plateau  $^{15}\text{NO}_3^-$  enrichment ranged from 4.26‰ (well I3) to 6.805‰ (well J2), while the stream water ranged from 9.935 to 10.092‰.

### 3.3. Temporal Dynamics of Hyporheic Transport and N Transformation

[21] Tracing  $\text{Cl}^-$  transport through the HZ generated median residence times ranging from 3.8 to 28.5 h (Figure 3). The shortest residence times were generally associated with the head of the gravel bar while the longest were located at the tail of the gravel bar. However, the longest median residence time (28.5 h) was observed at a midbar well, J1. Comparison of residence times to measured biogeochemical conditions (Figure 5) indicates that residence times less than 6.9 h were associated with a net dominance of oxic conditions and aerobic microbial processes ( $\text{O}_2$  respiration and nitrification) while residence times beyond 6.9 h were associated with a net dominance of hypoxic-anoxic conditions and anaerobic microbial processes (denitrification). More specifically, the greatest rates of DO, DOC, and  $\text{SUVA}_{254}$  reduction corresponded with the greatest rates of  $\text{NH}_3$  and  $\text{NO}_3^-$  production (Figure 5), all of which co-occurred during the first 6.9 h of observed transport. Beyond 6.9 h of residence time, DO, DOC, and  $\text{SUVA}_{254}$  continue to decrease gradually to a minimum of  $0.51 \text{ mg-O}_2 \text{ L}^{-1}$ ,  $1.66 \text{ mg-C L}^{-1}$ , and  $0.94 \text{ L mg-C}^{-1} \text{ m}^{-1}$ , respectively. Further,  $\text{SUVA}_{254}$  indicates that the highest fraction of labile DOC occurred when residence times were smallest, and that labile DOC was largely depleted by the time water attained larger residence times (Figure 5d).

[22] The concentration of  $^{15}\text{N}_2$  increased along proximal portions of flow paths with residence times  $< 3.8$  h, reaching a peak at the most distal portions of the flow paths where residence times exceeded 22 h (Figure 5f). The concentration of  $\text{NO}_3^-$  ( $\text{mg-N L}^{-1}$ ) also increased along the proximal portions of flow paths where residence times were less than 6.9 h, indicating concurrent nitrification and denitrification throughout the proximal portion of the gravel bar (Figure 5). Increases in  $\text{NH}_3$  were concurrent with consumption of DO and DOC (Figure 6). Comparison of DO and DOC concentrations with the conservative transport of  $\text{Cl}^-$  demonstrates that DO and DOC show net loss over all residence times (Figure 6). Conversely,  $\text{NH}_3$  shows net production until the very longest residence time of 28.5 h when it shows net loss, while  $\text{NO}_3^-$  shows net production until 18.2 h followed by net loss.

## 4. Discussion

[23] We utilized a whole-stream steady state  $^{15}\text{NO}_3^-$  and conservative tracer ( $\text{Cl}^-$ ) addition to observe spatial and temporal hydraulic and physiochemical conditions controlling  $\text{NO}_3^-$  dynamics in a HZ. Our results illustrate that nitrification and denitrification: (1) create nonlinear  $\text{NO}_3^-$  dynamic along HZ transport, (2) are not exclusively segregated processes in space and time, and (3) are strongly controlled by water and solute residence times in the HZ. From these findings we are able to confirm and build upon earlier conceptual frameworks [Jones and Holmes, 1996; Valett et al., 1996; Hedin et al., 1998] that relate HZ nitri-

fication and denitrification dynamics along flow paths and with residence times.

### 4.1. Spatial and Residence Time Dynamics of Hyporheic N

[24] Nitrate production versus removal can be site- and scale-dependent, and the hyporheic biogeochemistry in our study shows general spatial patterning in net N transformation processes consistent with earlier studies [e.g., Holmes et al., 1994; Pinay et al., 1994; Holmes et al., 1996]. The upgradient end of the HZ flow paths is dominated by oxic conditions and is a net  $\text{NO}_3^-$  production hot spot, while the middle and downgradient parts of the flow paths are anoxic and are a net  $\text{NO}_3^-$  removal hot spot (Figure 4). At the scale of the entire gravel bar, however, this HZ is a net  $\text{NO}_3^-$  removal hot spot for the stream. In contrast, other, smaller HZ units in the stream may be production hot spots because of their shorter flow paths and residence times. The residence time can be used to mark where this HZ turns from one redox condition to another: from net  $\text{NO}_3^-$  production to net  $\text{NO}_3^-$  removal (Figure 7). In this HZ, a water residence time of 6.9 h marks the threshold that separates these conditions. This observed threshold supports the HZ N transformation conceptual framework put forth by Jones and Holmes [1996] and Hedin et al. [1998]. The creation of this residence time threshold is complex and is a function of: (1) HZ water temperature (as it controls microbial activity and DO in water), (2) concentration of DO across the HZ (controlled by biological oxygen demand and advected supply), (3) HZ DOC supply and quality, (4) amount of  $\text{NO}_3^-$  in the HZ system, and (5) the physical hydraulics subsumed in the physical residence time of water (e.g., head gradient, hydraulic conductivity, advection, and dispersion).

[25] As shown in Figure 7, at times shorter than the threshold, transport and substrate conditions promote mineralization of stream sourced DON or particulate organic matter and subsequent nitrification with denitrification ( $\text{N}_2$  production) limited to microsite reactions [Sheibley et al., 2003]. As residence times increase, the extent of anaerobic water in the HZ grows and the effective nitrification rate decreases until its contribution to net  $\text{NO}_3^-$  production is negligible. At the threshold residence time, both processes are cooccurring and this is likely the location where the greatest rates of denitrification will be observed. Beyond the threshold, the HZ is dominated by net denitrification, and concentrations of both  $\text{NH}_3$  and  $\text{NO}_3^-$  decrease rapidly as denitrification is not substrate (labile DOC) limited and  $\text{NO}_3^-$  production rapidly decreases. Finally, at much longer residence times, the rate of denitrification will decrease due to an increasing DOC substrate limitation and lack of  $\text{NO}_3^-$ , even though redox conditions remain appropriate to carry out denitrification.

[26] Similar nitrification-denitrification coupling has been observed in stream HZs where DON-rich anoxic ground-water flows into oxic stream sediments [e.g., Hedin et al., 1998; Sheibley et al., 2003]. The thermodynamic framework of Hedin et al. [1998] clearly illustrates that microbial redox processes, including nitrification-denitrification, will be tightly coupled in the riparian and hyporheic environments where solutes exchange across oxic-anoxic boundaries. Our study illustrates this tight coupling occurs in space and time as shown by the spatial distribution of N species

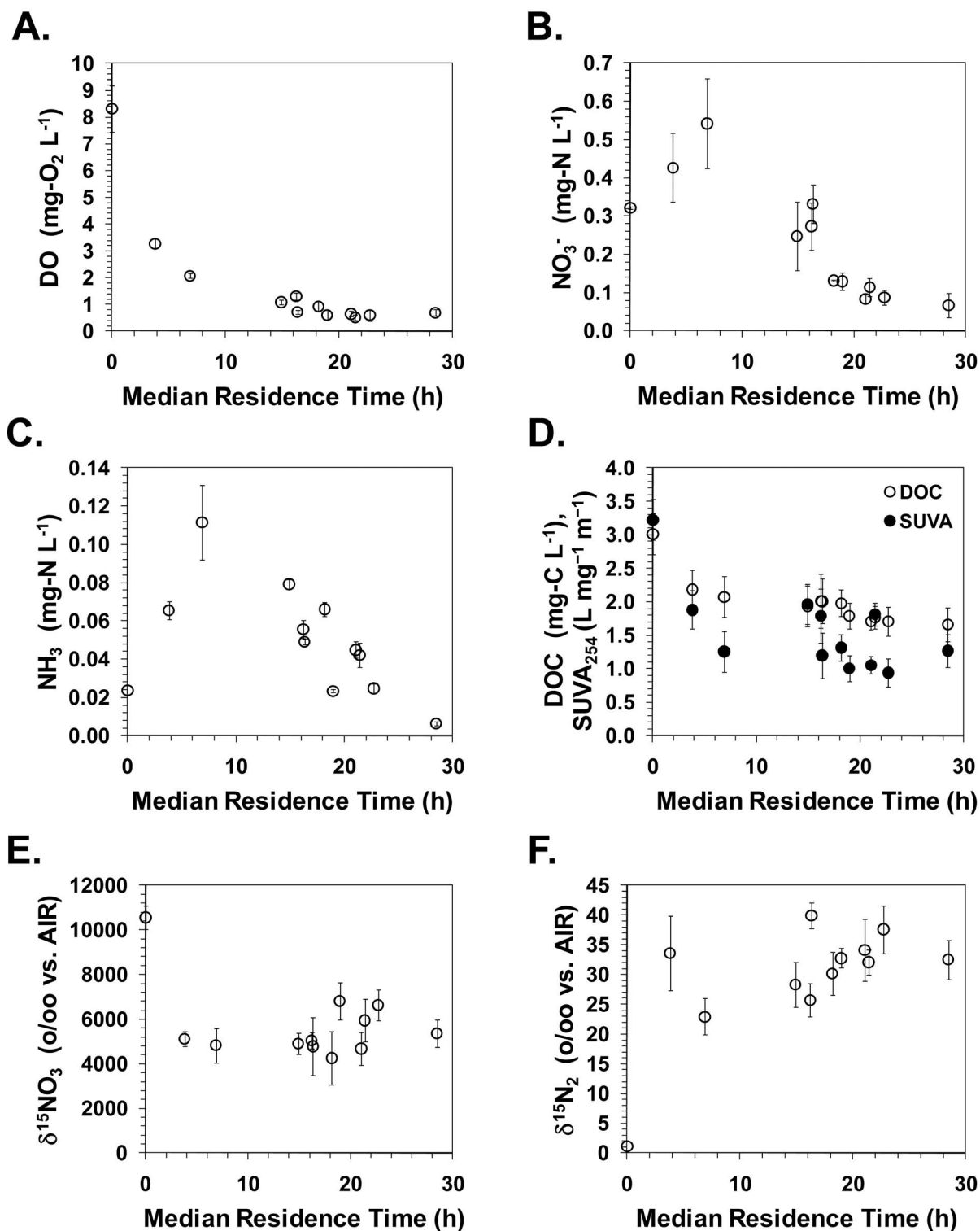


**Figure 5.** Steady state hyporheic zone biogeochemical and <sup>15</sup>N conditions relative to median residence time: (a) dissolved oxygen (DO), (b) nitrate (NO<sub>3</sub><sup>-</sup>), (c) ammonia (NH<sub>3</sub>), (d) total dissolved organic carbon (DOC) with SUVA<sub>254</sub>, (e) δ<sup>15</sup>N-nitrate (δ<sup>15</sup>N-NO<sub>3</sub><sup>-</sup>), and (f) δ<sup>15</sup>N-dinitrogen (δ<sup>15</sup>N-N<sub>2</sub>). Each data point represents the mean values generated from repeated samples ( $n = 5$ , error bars =  $\pm 2$  standard error) collected during tracer plateau conditions. Stream water values are shown as a median residence time = 0 h.



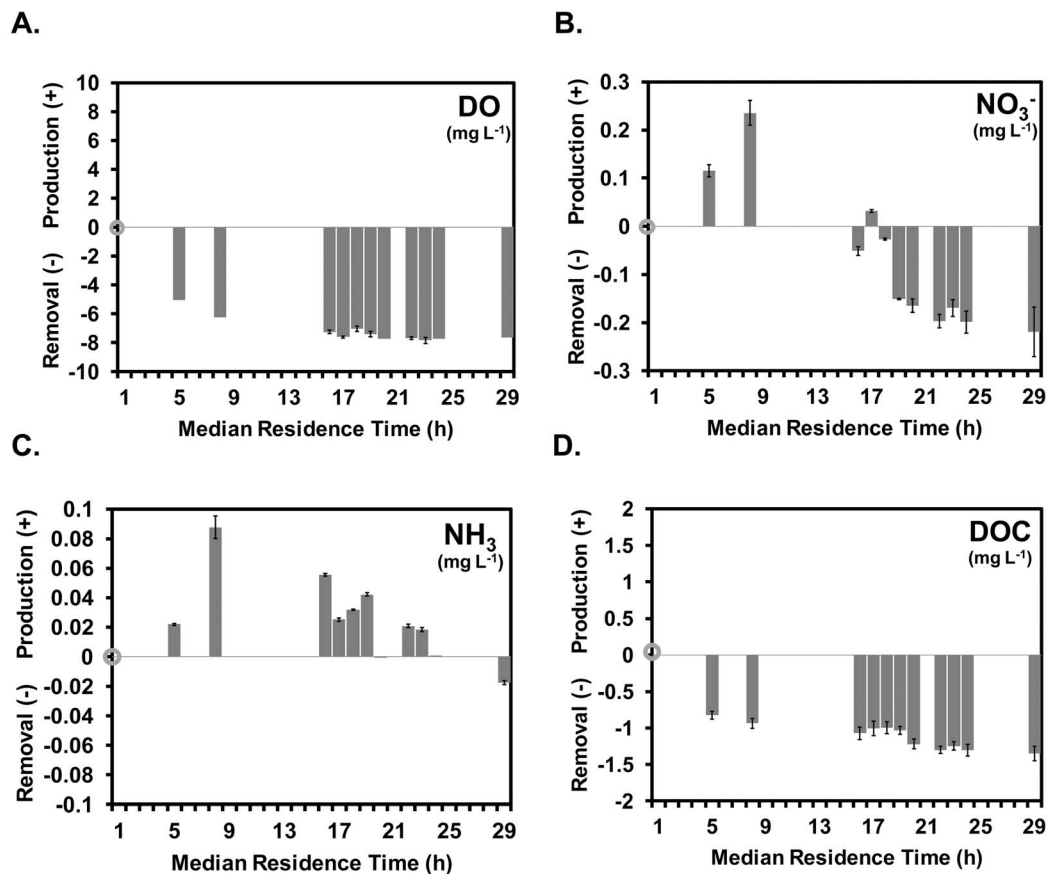


**Figure 6.** Apparent net production and removal based upon conservative transport relative to median residence time for: (a) dissolved oxygen (DO), (b) nitrate ( $\text{NO}_3^-$ ), (c) ammonia ( $\text{NH}_3$ ), and (d) total dissolved organic carbon (DOC). Positive values represent production, negative values represent removal, and the zero line represents conservative transport of compound. Each data point represents the mean values generated from repeated samples ( $n = 5$ , error bars =  $\pm 2$  standard error) collected during tracer plateau conditions.

(Figure 4) and the residence time threshold between net nitrification and denitrification (Figure 7). This suggests that a thermodynamic approach is useful and should be coupled to physical transport dynamics in order to better understand the spatial and temporal distribution of different hyporheic redox environments.

[27] Earlier studies [e.g., Valett *et al.*, 1996; Pinay *et al.*, 2009] indicate that biologically mediated N fluxes through the HZ are explicitly a function of HZ flow path length and implicitly a function of residence time (i.e., space for time [see Jones and Holmes, 1996, and references therein]). In this study,  $^{15}\text{N}$  tracing explicitly shows that there is a relationship between N fluxes and HZ residence time. Earlier studies by Valett *et al.* [1996] and Pinay *et al.* [2009] collected measures of HZ solute transit times during their N addition experiments and found that  $\text{NO}_3^-$  uptake and denitrification were the dominant N transformations processes. However, they did not observe the coupling of nitrification and denitrification (i.e., nitrification preceding denitrification along increasing residence times). In their studies,  $\text{NO}_3^-$  uptake and denitrification processes occurred across all measured transport times achieving maximums during the first 1.7 h of travel time. Conversely, our study shows a

different N removal pattern, one that is more complex, with nitrification occurring at short residence times and denitrification at late residence times (Figures 6 and 7). A main difference between our study and these earlier studies is the use of  $^{15}\text{NO}_3^-$  to trace N dynamics under near ambient  $\text{NO}_3^-$  conditions. Valett *et al.* [1996] and Pinay *et al.* [2009] elevated  $\text{NO}_3^-$  concentrations in their HZ studies (6.4- to 24-fold  $\text{NO}_3^-$  increase, respectively).  $\text{NO}_3^-$  transformations are concentration-dependent, and elevated  $\text{NO}_3^-$  conditions can increase rates of HZ uptake and denitrification [Jones and Holmes, 1996]. Consequently, the use of  $^{15}\text{NO}_3^-$  allowed us to observe different  $\text{NO}_3^-$  transformations under approximately ambient concentrations.

[28] In addition to  $\text{NO}_3^-$  removal via denitrification, bacterial assimilation is an important N retention process and may account for a significant fraction of the observed DOC and  $\text{NO}_3^-$  removal across the HZ. Following Sobczak *et al.* [2003], using the observed DOC loss across the HZ =  $1.35 \text{ mg-C L}^{-1}$ , and assuming a microbial growth efficiency of 50% and a microbial C:N = 7:1, a potential  $0.68 \text{ mg-C L}^{-1}$  and  $0.1 \text{ mg-N L}^{-1}$  could be assimilated into microbial biomass. Under these assumptions, microbial assimilation can

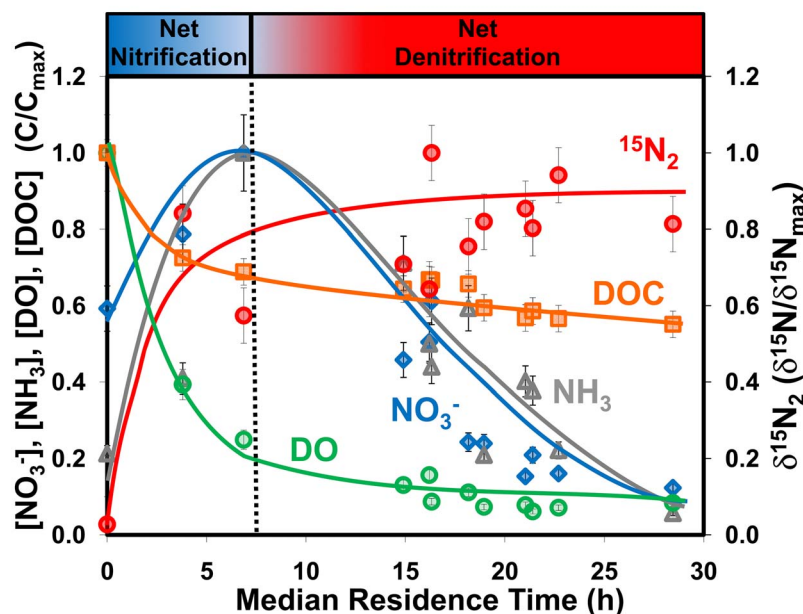


**Figure 7.** Conceptual model showing a continuum between net hyporheic nitrification and denitrification conditions (labeled lines) as a function residence time. Note that the conceptual model is overlaid on the observed steady state nitrification-denitrification species, dissolved organic carbon, and dissolved oxygen conditions: dissolved oxygen (DO, green circles), nitrate ( $\text{NO}_3^-$ , blue diamonds), ammonia ( $\text{NH}_3$ , gray triangles), total dissolved organic carbon (DOC, orange squares), and  $\delta^{15}\text{N}_2$ -dinitrogen ( $\delta^{15}\text{N}_2$ , red circles). Each data point represents the normalized mean values generated from repeated plateau samples ( $n = 5$ , error bars =  $\pm 2$  standard error, values were normalized by maximum observed concentration or  $^{15}\text{N}$  enrichment).

account for 21% of the  $\text{NO}_3^-$  loss across the gravel bar HZ. This microbial assimilation of  $\text{NO}_3^-$  is supported by the lower  $^{15}\text{N}$  enrichment values observed in the HZ  $^{15}\text{NO}_3^-$  compared to the stream surface waters (Figure 4). Both microbial assimilation and denitrification will act to lower  $^{15}\text{N}$  enrichment of the HZ  $^{15}\text{NO}_3^-$  pool. After accounting for assimilation of  $\text{NO}_3^-$ , the respiratory denitrification may account for as much as 79% of the total  $\text{NO}_3^-$  removed from stream water flowing through the HZ of this gravel bar.

[29] DOC quantity and quality also clearly depend on residence time. This is expected given the role DOC plays as a substrate for the observed nitrification and denitrification. Previous work has demonstrated a strong positive relationship between DOC loss and bacterial productivity along hyporheic flow paths [Sobczak and Findlay, 2002]. The concurrent declines in DOC and DO concentration with increasing flow path length and residence times indicates strong aerobic metabolism in this gravel bar HZ. Similar observations of DOC declines were also seen along flow path length in the controlled mesocosm experiments of Sobczak *et al.* [2003]; they found that the DOC dynamics were a function of rapid microbial utilization of the bioavailable fractions of the DOC followed by conservative transport of the unavailable DOC fraction. In this study, we are able to relate these DOC spatial dynamics to transport times. In doing so, we see the same conservative transport of the less labile fraction of the DOC at longer flow paths and residence times (Figure 5d); however, some labile DOC

must be present at later residence times to provide necessary substrate for denitrification.

#### 4.2. The $^{15}\text{N}$ Tracing Shows Overlapping N Process Domains

[30] At the organismal level, microbial denitrification requires anoxic conditions. However, it is well known that denitrification can occur in anoxic biofilms within bulk conditions that are oxic [e.g., Holmes *et al.*, 1996]. Hence, it is possible for denitrification and nitrification to proceed concurrently in a small volume of the HZ. Our observation of  $^{15}\text{N}_2$  production at wells exhibiting net  $\text{NO}_3^-$  production (Figure 7) indicates that over short residence times the water has encountered denitrification microsites in less mobile pore water. When low-flow water samples were collected from wells, water and solutes were accessed from both mobile and immobile domains, as seen in other groundwater well sampling regimes [e.g., Harvey and Gorelick, 2000]. In the case of our study, at short residence times, the advection-dominated mobile domain likely supports the aerobic processes and the diffusion-dominated immobile domain supports anaerobic processes. In contrast, at long residence times both mobile and immobile domains become anoxic as the DO is utilized along the flow path. The use of  $^{15}\text{N}$  tracing permitted us to see that a HZ water sample contains signals from multiple distinct N transformation domains. This overlapping domain complexity can be accounted for with a residence time distribution perspective, because the residence time distribution of sample volume integrates the

effect of different process domains encountered during hyporheic transport (e.g., large subsurface heterogeneity and gradients created by advective-dispersive transport, mixing flow paths, or substrate patchiness).

[31] Future work should explore the role of these overlapping process domains in light of other possible explanations that we are unable to address with the current study. For example, labile DOC subsurface heterogeneity can also generate spatial and temporal N transformation heterogeneity. Another issue is that rapid localized redox condition changes could be created while drawing the low-flow water sample. During the sampling, an otherwise anoxic region in the HZ around the well may have more oxic water drawn into the well via the pumping of upgradient preferential flow paths. In this case, a denitrification signal from the anoxic pore waters surrounding the well will be combined with the upgradient waters properties such as higher DO concentrations and nitrification.

## 5. Conclusions

[32] Results from the coupled conservative and  $^{15}\text{N}$  reactive tracer experiment provide definitive evidence of in situ denitrification occurring in the HZ. Further, the comparison between conservative tracer and reactive  $^{15}\text{N}$  tracers enable us to relate the fate and transport of DO, DOC, and  $\text{NO}_3^-$  to water residence times. In this hyporheic zone, short residence times were dominated by aerobic metabolic processes such as the rapid utilization of DO and DOC and the production of ammonia and nitrate (ammonification and nitrification, respectively). However, a clear denitrification signal, concurrent in both space and time, was also observed during short residence times indicating anaerobic microsites. Beyond a residence time threshold of 6.9 h in this HZ, the anaerobic metabolic process of denitrification dominated the system, and resulted in a net removal of nitrate from the stream. Thus, this HZ was a hot spot for nitrogen transformation, where hot spots of nitrate production and removal were distinguished by residence time.

[33] In this gravel bar HZ, the combination of  $^{15}\text{N}$  tracing with a relatively elegant, highly instrumented hydrologic system (Figure 1), we see that residence time helps make N transformation relationships more clear (Figure 7). The actual spatial and temporal location of the threshold between net N transformation process domains is expected to vary between representative HZ units given their exact combination of hydrologic and upgradient biogeochemical and substrate characteristics. Further, this threshold is likely to vary in time with daily and seasonal changes in hydraulic, temperature, and water chemistry conditions. Ultimately, relating hyporheic denitrification controls to residence times will help to upscale denitrification measurements to stream reach and network scales in a way that is linked quantitatively to transient storage.

[34] **Acknowledgments.** Support for this project was provided via NSF grant EAR-041240 to R.H., S.M.W., and M.A.B. and NSF grant DGE-0333257 and OSU Institute for Water and Watersheds (IWW) grant to J.P.Z. Further support was provided by the Hollis M. Dole Environmental Geology Fund at OSU. Any opinions, findings, and conclusions or recommendations expressed in this material are those of the authors and do not necessarily reflect the views of the NSF. We thank the associate editor and two anonymous reviewers whose comments improved

this manuscript. Special thanks to: V. Adams, S. Baxter, P. Zarnetske, A. Argerich, and B. Burkholder for field/lab assistance; L. Ashkenas and S. Thomas for advising J.P.Z. on stable  $^{15}\text{N}$  handling; M. Otter of MBL's Stable Isotope Laboratory for analyzing  $^{15}\text{N}$  samples; and C. Jones and K. Motter of CCAL and OSU IWW Collaboratory for help with analyzing general water chemistry.

## References

- Alexander, R. B., et al. (2000), Effect of stream channel size on the delivery of nitrogen to the Gulf of Mexico, *Nature*, *403*, 758–761, doi:10.1038/35001562.
- Anderson, J. K., et al. (2005), Patterns in stream longitudinal profiles and implications for hyporheic exchange flow at the H. J. Andrews Experimental Forest, Oregon, USA, *Hydrol. Process.*, *19*, 2931–2949, doi:10.1002/hyp.5791.
- Baker, M. A., et al. (1999), Acetate retention and metabolism in the hyporheic zone of a mountain stream, *Limnol. Oceanogr.*, *44*, 1530–1539, doi:10.4319/lo.1999.44.6.1530.
- Baker, M. A., et al. (2000), Organic carbon supply and metabolism in a shallow groundwater ecosystem, *Ecology*, *81*, 3133–3148, doi:10.1890/0012-9658(2000)081[3133:OCSAMI]2.0.CO;2.
- Böhlke, J. K., et al. (2004), Reach-scale isotope tracer experiment to quantify denitrification and related processes in a nitrate-rich stream, midcontinent United States, *Limnol. Oceanogr.*, *49*, 821–838, doi:10.4319/lo.2004.49.3.0821.
- Böhlke, J. K., et al. (2009), Multi-scale measurements and modeling of denitrification in streams with varying flow and nitrate concentration in the upper Mississippi River basin, USA, *Biogeochemistry*, *93*, 117–141, doi:10.1007/s10533-008-9282-8.
- Clilverd, H. M., et al. (2008), Nitrogen retention in the hyporheic zone of a glacial river in interior Alaska, *Biogeochemistry*, *88*, 31–46, doi:10.1007/s10533-008-9192-9.
- Diaz, R. J., and R. Rosenberg (2008), Spreading dead zones and consequences for marine ecosystems, *Science*, *321*, 926–929, doi:10.1126/science.1156401.
- Duff, J. H., and F. J. Triska (2000), Nitrogen biogeochemistry and surface-subsurface exchange in streams, in *Streams and Ground Waters*, edited by J. A. Jones and P. J. Mulholland, pp. 197–217, Academic, San Diego, Calif.
- Duff, J. H., et al. (1996), Nitrate reduction in sediments of lowland tropical streams draining swamp forest in Costa Rica: An ecosystem perspective, *Biogeochemistry*, *33*, 179–196, doi:10.1007/BF02181071.
- Findlay, S. (1995), Importance of surface-subsurface exchange in stream ecosystems: The hyporheic zone, *Limnol. Oceanogr.*, *40*, 159–164, doi:10.4319/lo.1995.40.1.0159.
- Gu, C. H., G. M. Hornberger, A. L. Mills, J. S. Herman, and S. A. Flewelling (2007), Nitrate reduction in streambed sediments: Effects of flow and biogeochemical kinetics, *Water Resour. Res.*, *43*, W12413, doi:10.1029/2007WR006027.
- Hamilton, S. K., and N. E. Ostrom (2007), Measurement of the stable isotope ratio of dissolved N-2 in N-15 tracer experiments, *Limnol. Oceanogr. Methods*, *5*, 233–240.
- Harvey, C. F., and S. M. Gorelick (2000), Rate-limited mass transfer or macrodispersion: Which dominates plume evolution at the Macrodispersion Experiment (MADE) site?, *Water Resour. Res.*, *36*, 637–650, doi:10.1029/1999WR900247.
- Hedin, L. O., et al. (1998), Thermodynamic constraints on nitrogen transformations and other biogeochemical processes at soil-stream interfaces, *Ecology*, *79*, 684–703.
- Henry, J., and S. Fisher (2003), Spatial segregation of periphyton communities in a desert stream: Causes and consequences for N cycling, *J. N. Am. Benthol. Soc.*, *22*, 511–527, doi:10.2307/1468349.
- Hill, A. R., and D. J. Lyburner (1998), Hyporheic zone chemistry and stream-subsurface exchange in two groundwater-fed streams, *Can. J. Fish. Aquat. Sci.*, *55*, 495–506, doi:10.1139/cjfas-55-2-495.
- Holmes, R. M., et al. (1994), Parafluvial nitrogen dynamics in a desert stream ecosystem, *J. N. Am. Benthol. Soc.*, *13*, 468–478, doi:10.2307/1467844.
- Holmes, R. M., et al. (1996), Denitrification in a nitrogen-limited stream ecosystem, *Biogeochemistry*, *33*, 125–146, doi:10.1007/BF02181035.
- Jones, J. B., and R. M. Holmes (1996), Surface-subsurface interactions in stream ecosystems, *Trends Ecol. Evol.*, *11*, 239–242, doi:10.1016/0169-5347(96)10013-6.
- Jones, J. B., S. G. Fisher, and N. B. Grimm (1995), Nitrification in the hyporheic zone of a desert stream ecosystem, *J. N. Am. Benthol. Soc.*, *14*, 249–258, doi:10.2307/1467777.
- Kaplan, L. A., and J. D. Newbold (2000), Surface and subsurface dissolved organic carbon, in *Streams and Ground Waters*, edited by J. A. Jones and P. J. Mulholland, pp. 237–253, Academic, San Diego, Calif.

- McClain, M. E., et al. (2003), Biogeochemical hot spots and hot moments at the interface of terrestrial and aquatic ecosystems, *Ecosystems*, 6, 301–312, doi:10.1007/s10021-003-0161-9.
- Montgomery, D. R., and J. M. Buffington (1997), Channel-reach morphology in mountain drainage basins, *Geol. Soc. Am. Bull.*, 109, 596–611, doi:10.1130/0016-7606(1997)109<0596:CRMIMD>2.3.CO;2.
- Morrice, J. A., et al. (2000), Terminal electron accepting processes in the alluvial sediments of a headwater stream, *J. N. Am. Benthol. Soc.*, 19, 593–608, doi:10.2307/1468119.
- Mulholland, P. J., et al. (2004), Stream denitrification and total nitrate uptake rates measured using a field N-15 tracer addition approach, *Limnol. Oceanogr.*, 49, 809–820, doi:10.4319/lo.2004.49.3.0809.
- Mulholland, P. J., et al. (2008), Stream denitrification across biomes and its response to anthropogenic nitrate loading, *Nature*, 452, 202–205, doi:10.1038/nature06686.
- Peterson, B. J., et al. (2001), Control of nitrogen export from watersheds by headwater streams, *Science*, 292, 86–90, doi:10.1126/science.1056874.
- Pinay, G., et al. (1994), The role of denitrification in nitrogen removal in river corridors, in *Global Wetlands: Old World and New*, edited by W. J. Mitsch, pp. 107–116, Elsevier, Amsterdam.
- Pinay, G., et al. (2009), Nitrate removal in the hyporheic zone of a salmon river in Alaska, *River Res. Appl.*, 25, 367–375, doi:10.1002/rra.1164.
- Schlesinger, W. H., et al. (2006), Global change: The nitrogen cycle and rivers, *Water Resour. Res.*, 42, W03S06, doi:10.1029/2005WR004300.
- Seitzinger, S. P. (1988), Denitrification in freshwater and coastal marine ecosystems: Ecological and geochemical significance, *Limnol. Oceanogr.*, 33, 702–724, doi:10.4319/lo.1988.33.4\_part\_2.0702.
- Sheibley, R. W., et al. (2003), Numerical modeling of coupled nitrification-denitrification in sediment perfusion cores from the hyporheic zone of the Shingobee River, MN, *Adv. Water Resour.*, 26, 977–987, doi:10.1016/S0309-1708(03)00088-5.
- Sigman, D. M., et al. (1997), Natural abundance-level measurement of the nitrogen isotopic composition of oceanic nitrate: An adaptation of the ammonia diffusion method, *Mar. Chem.*, 57, 227–242, doi:10.1016/S0304-4203(97)00009-1.
- Sobczak, W. V., and S. Findlay (2002), Variation in bioavailability of dissolved organic carbon among stream hyporheic flowpaths, *Ecology*, 83, 3194–3209, doi:10.1890/0012-9658(2002)083[3194:VIBODO]2.0.CO;2.
- Sobczak, W. V., et al. (2003), Relationships between DOC bioavailability and nitrate removal in an upland stream: An experimental approach, *Biogeochemistry*, 62, 309–327, doi:10.1023/A:1021192631423.
- Triska, F. J., et al. (1993), The role of water exchange between a stream channel and its hyporheic zone in nitrogen cycling at the terrestrial-aquatic interface, *Hydrobiologia*, 251, 167–184, doi:10.1007/BF00007177.
- Valett, H. M., S. G. Fisher, N. B. Grimm, and P. Camill (1994), Vertical hydrologic exchange and ecological stability of a desert stream ecosystem, *Ecology*, 75, 548–560, doi:10.2307/1939557.
- Valett, H. M., et al. (1996), Parent lithology, surface-groundwater exchange, and nitrate retention in headwater streams, *Limnol. Oceanogr.*, 41, 333–345, doi:10.4319/lo.1996.41.2.0333.
- Weishaar, J. L., et al. (2003), Evaluation of specific ultraviolet absorbance as an indicator of the chemical composition and reactivity of dissolved organic carbon, *Environ. Sci. Technol.*, 37, 4702–4708, doi:10.1021/es030360x.
- Woessner, W. W. (2007), Building a compact, low-cost, and portable peristaltic sampling pump, *Ground Water*, 45, 795–797, doi:10.1111/j.1745-6584.2007.00346.x.
- Wondzell, S. M., and F. J. Swanson (1996), Seasonal and storm dynamics of the hyporheic zone of a 4th-order mountain stream. 2. Nitrogen cycling, *J. N. Am. Benthol. Soc.*, 15, 20–34, doi:10.2307/1467430.

M. A. Baker, Department of Biology, Utah State University, Logan, UT 84322, USA.

R. Haggerty and J. P. Zarnetske, Department of Geosciences, Oregon State University, Corvallis, OR 97331, USA. (zarnetsj@geo.oregonstate.edu)

S. M. Wondzell, Olympia Forestry Sciences Laboratory, Pacific Northwest Research Station, Olympia, WA 98512, USA.